Modeling nuclear fusion in dense plasmas using a cryogenic non-neutral plasma[a)]

Daniel H. E. Dubin[b)]
Department of Physics, University of California at San Diego, La Jolla, California 92093, USA

An analogy between the nuclear reaction rate in a dense neutral plasma and the energy equipartition rate in a strongly magnetized non-neutral plasma is discussed. This analogy allows the first detailed measurements of plasma screening enhancements in the strong screening and pycnonuclear regimes. In strong magnetic fields and at low temperatures, cyclotron energy, like nuclear energy, is released only through rare close collisions between charges. The probability of such collisions is enhanced by plasma screening, just as for nuclear reactions. Rate enhancements of up to 10^{10} are measured in simulations of equipartition, and are compared to theories of screened nuclear reactions. © *2008 American Institute of Physics*. [DOI: 10.1063/1.2844370]

I. INTRODUCTION

This paper will describe theory and simulations that use a non-neutral plasma to model aspects of the physics of nuclear fusion reactions in dense plasmas, such as occur in degenerate stars, giant planet interiors, and inertially confined laser fusion plasmas. In such plasmas, the Coulomb coupling parameter $\Gamma \equiv e^2/aT$ can approach, or even exceed, unity. (Here e is the charge of individual nuclei, assumed identical for simplicity, T is the temperature in energy units, and a is the Wigner–Seitz radius defined in terms of the plasma number density n_0 as $4\pi a^3 n_0/3 = 1$.)

Nuclear reaction rates in dense plasmas are predicted to be enhanced compared to the rates predicted for reactions at low densities.[1–13] The enhancement is caused by plasma screening of the repulsive Coulomb potential between nuclei, which allows them to have closer collisions for a given relative energy. This plasma screening enhancement of nuclear reaction rates is predicted to be very large when the plasma is strongly coupled, and this has important implications for a range of physical processes in dense plasmas. However, the twin requirements of high plasma temperature (for measurable nuclear reaction rates) and high density (for strong coupling) make laboratory measurements of large plasma screening enhancements exceptionally difficult. For example, in a typical white dwarf with $n = 10^{30}$ cm^{-3} and $T = 10^6$ K, a helium plasma is moderately strongly coupled with $\Gamma \cong 40$, but the plasma pressure (due mostly to the degenerate electrons) is on the order of 10^{17} atmospheres, well beyond current laboratory capabilities.

This paper examines an analogy between screened nuclear reactions in dense plasmas and energy equipartition in a strongly coupled and strongly magnetized non-neutral plasma. The analogy allows the measurement of large plasma screening enhancements and comparison to theory predictions of the enhancements for the first time.

When a non-neutral plasma is at sufficiently low temperature T and is in a sufficiently strong magnetic field B, the cyclotron frequency $\Omega_c = eB/mc$ can be the highest dynamical frequency, higher even than the frequency $\bar{v}/\bar{b}$ associated with typical collisions. (Here $\bar{v} = \sqrt{T/m}$ is the thermal speed and $\bar{b} = e^2/T$ is the mean distance of closest approach.) In this "strongly magnetized" regime where the mean "adiabaticity parameter" $\bar{\kappa} \equiv \sqrt{2}\Omega_c \bar{b}/\bar{v} \gg 1$, the total cyclotron energy $E_\perp = \Sigma_{i=1}^N m v_{\perp i}^2/2$ (where $\mathbf{v}_{\perp i}$ is the velocity perpendicular to $\mathbf{B}$ of the ith charge) is an adiabatic invariant.[14,15] Cyclotron energy is shared with motion parallel to $\mathbf{B}$ only through rare close collisions that break the adiabatic invariant. Thus, cyclotron energy is analogous to the energy stored in nuclei, which can also be released only through close collisions.

The rate at which cyclotron energy is released, i.e., the rate ν of equipartition of perpendicular temperature $T_\perp$ and parallel temperature T, is enhanced by plasma screening. Thus, the rate of equipartition in a strongly magnetized non-neutral plasma is analogous to the nuclear reaction rate in a dense neutral plasma. Weak screening, strong screening, and pycnonuclear regimes can be identified that are analogous to those for nuclear reactions.

Furthermore, we will see that in the weak and strong screening regimes, the enhancement factor to the equipartition rate is identical to the enhancement to the nuclear reaction rate, because both processes are dominated by close collisions that become more likely when plasma screening is taken into account.

The rate of collisional equipartition in the strongly magnetized regime has been previously measured in cryogenic pure electron plasmas,[16] and shows quantitative agreement with theory.[14,15] More recent experiments with cryogenic pure ion plasmas have also observed this equipartition, and these experiments have extended into regimes of strong correlation.[17,18] It is possible that these experiments will also make quantitative comparisons to theory. In this paper, we focus on the analytic theory and on simulations as "experiments" to corroborate the theory.

15, 055705-1

II. THEORY OF EQUIPARTITION IN A STRONGLY MAGNETIZED NON-NEUTRAL PLASMA

In this section, we present a brief review of the physics of energy equipartition in a strongly magnetized non-neutral plasma. We first review the original theory of O'Neil and Hjorth[14] and Glinsky et al.[15] that neglects plasma screening, and we then consider screening effects.

The first step in the calculation of the equipartition rate is to analyze the collisional dynamics of an isolated pair of like charges in a strong uniform magnetic field $\mathbf{B} = B\hat{z}$. The equations of motion for the two charges are

$$\frac{d\mathbf{v}_1}{dt} = \frac{e^2}{m} \frac{(\mathbf{r}_1 - \mathbf{r}_2)}{|\mathbf{r}_1 - \mathbf{r}_2|^3} + \Omega_c \mathbf{v}_1 \times \hat{z}, \tag{1}$$

$$\frac{d\mathbf{v}_2}{dt} = \frac{e^2}{m} \frac{(\mathbf{r}_2 - \mathbf{r}_1)}{|\mathbf{r}_1 - \mathbf{r}_2|^3} + \Omega_c \mathbf{v}_2 \times \hat{z}, \tag{2}$$

where $\mathbf{r}_i$ and $\mathbf{v}_i$ are the positions and velocities of charge i. Adding and subtracting these equations yields equations for the center of mass velocity $\mathbf{V} = (\mathbf{v}_1 + \mathbf{v}_2)/2$ and the relative velocity $\mathbf{v} = \mathbf{v}_2 - \mathbf{v}_1$,

$$\frac{d\mathbf{V}}{dt} = \Omega_c \mathbf{V} \times \hat{z}, \tag{3}$$

$$\frac{d\mathbf{v}}{dt} = \frac{e^2}{\mu} \frac{\mathbf{r}}{|r|^3} + \Omega_c \mathbf{v} \times \hat{z}, \tag{4}$$

where $\mu = m/2$ is the reduced mass and $\mathbf{r} = \mathbf{r}_2 - \mathbf{r}_1$ is the displacement between the charges. Thus, the center of mass motion does not affect the relative motion, and each can be considered separately. Furthermore, one can see from Eq. (3) that $V_\perp^2(t)$ is an exact constant of the motion. We will now see that $v_\perp^2(t)$ is an approximate constant of the motion (an adiabatic invariant) when the dynamics is strongly magnetized. This in turn implies that $E_\perp = mv_{\perp 1}^2/2 + mv_{\perp 2}^2/2$ is also an adiabatic invariant, since $E_\perp$ can also be written as

$$E_\perp = \mu v_\perp^2/2 + 2mV_\perp^2/2. \tag{5}$$

By taking the dot product of Eq. (4) with $\mathbf{v}_\perp$, we obtain the following expression for the rate of change of $v_\perp^2(t)$:

$$\frac{d}{dt}\left(\frac{\mu v_\perp^2}{2}\right) = \frac{e^2 \mathbf{v}_\perp(t) \cdot \mathbf{r}(t)}{|r|^3}. \tag{6}$$

Thus, the total change is $v_\perp^2$ over the course of a collision is

$$\Delta v_\perp^2 = \frac{2e^2}{\mu} \int_{-\infty}^{\infty} dt \frac{\mathbf{v}_\perp(t) \cdot \mathbf{r}(t)}{|r|^3}. \tag{7}$$

The value of the integral can be estimated by using approximate orbits based on guiding-center dynamics,

$$\Delta v_\perp^2 \simeq \frac{2e^2}{\mu} v_\perp \rho \int_{-\infty}^{\infty} dt \frac{\cos(\Omega_c t + \phi)}{(\rho^2 + z^2(t))^{3/2}}, \tag{8}$$

where $(\boldsymbol{\rho}, z)$ is the guiding center approximation for $(\mathbf{r}_\perp, z)$, and ϕ is a (constant) phase factor. The relative position in z, $z(t)$, is determined by energy conservation of the parallel

motion (neglecting the change in $v_\perp^2(t)$, which is assumed small),

$$\frac{\mu}{2}\dot{z}^2(t) + \frac{e^2}{(\rho^2 + z(t)^2)^{1/2}} = \frac{\mu}{2}\dot{z}^2(t = -\infty) \equiv E_\parallel \equiv \frac{\mu}{2}v_\parallel^2. \tag{9}$$

By suitably scaling distances and times, Eq. (8) can be written as

$$\Delta v_\perp^2 = \frac{2e^2}{\mu} \frac{v_\perp \rho}{b^2 v_\parallel} \cos\phi \, f(\rho/b, \kappa), \tag{10}$$

where $b \equiv e^2/E_\parallel$ is the distance of closest approach for a collision with initial relative parallel energy $E_\parallel = \mu v_\parallel^2/2$, $\kappa = b\Omega_c/v_\parallel$ is the adiabaticity parameter for such a collision, and

$$f(\bar{\rho}, \kappa) = \int_{-\infty}^{\infty} \frac{d\bar{t} \cos(\kappa \bar{t})}{(\bar{\rho}^2 + \bar{z}^2(\bar{t}))^{3/2}}, \tag{11}$$

where $\bar{z}(t)$ satisfies the scaled version of Eq. (9),

$$\dot{\bar{z}}^2 + \frac{1}{(\bar{\rho}^2 + \bar{z}^2)^{1/2}} = 1. \tag{12}$$

The function $f(\bar{\rho}, \kappa)$ has the following asymptotic form when $\kappa \gg 1$:

$$f(\bar{\rho}, \kappa) = h(\bar{\rho}, \kappa) e^{-g(\rho)\kappa}, \tag{13}$$

where $h(\bar{\rho}, \kappa)$ is neither exponentially small nor large in the region of interest, and $g(\rho)$ is an increasing function of ρ, with $g(0) = \pi/2$.[14] Thus, for large κ, $\Delta v_\perp^2$ is exponentially small, taking its largest value at fixed κ for head-on collisions with $\rho = 0$.

Now consider the effect of many such collisions occurring in a uniform plasma of density n, with parallel temperature T and perpendicular temperature $T_\perp$. The collisions eventually bring $T_\perp$ and T into equipartition, according to the equation

$$\frac{dT_\perp}{dt} = \nu(T - T_\perp), \tag{14}$$

where ν is the rate of equipartition. O'Neil and Hjorth showed that ν can be written as an integral over a Maxwellian distribution of relative parallel energies $E_\parallel = \mu v_\parallel^2/2$ and a differential rate $\sigma(E_\parallel)$ that depends quadratically on $\Delta v_\perp^2$,

$$\nu_0 = \int \frac{dE_\parallel}{T} e^{-E_\parallel/T} \sigma(E_\parallel), \tag{15}$$

where

$$\sigma(E_\parallel) = \frac{n}{16\pi T_\perp^2} \frac{\mu^2}{(2\pi T/\mu)^{1/2}} \int d^2\rho \, d^2 v_\perp (\Delta v_\perp^2)^2 e^{-\mu v_\perp^2/2T_\perp}$$

$$= \frac{\pi}{2} \frac{ne^4}{\mu E_\parallel \sqrt{2\pi T/\mu}} \int_0^{\infty} d\bar{\rho}\bar{\rho}^3 f^2(\bar{\rho}, \kappa). \tag{16}$$

In Eq. (15), the notation ν_0 is used to indicate that screening effects are neglected. The function $\sigma(E_\parallel)$ is rapidly increasing as $E_\parallel$ increases, due to the exponential in Eq. (13),

$$\sigma(E_{\parallel}) = \frac{\pi}{2} \frac{ne^4}{\mu E_{\parallel}\sqrt{2\pi T/\mu}} s(\kappa)e^{-\pi\kappa}, \tag{17}$$

where $s(\kappa)$ is a relatively slowly varying function compared to the exponential.

The combination of the decreasing Maxwellian and the exponentially increasing function σ in Eq. (15) leads to a sharp peak in the integrand, at an energy E_G determined by

$$\frac{\partial}{\partial E_{\parallel}} e^{-E_{\parallel}/T_{\parallel} - \pi\kappa}\bigg|_{E_{\parallel}=E_G} = 0. \tag{18}$$

This energy, analogous to the Gamow energy in nuclear reactions, is found from Eq. (18) to be

$$E_G = \left(\frac{3\pi}{4\sqrt{2}}\bar{\kappa}\right)^{2/5} T, \tag{19}$$

where

$$\bar{\kappa} \equiv \sqrt{2}\bar{b}\Omega_c/\bar{v} = 1070(B/1\text{ T})\left(\frac{m}{m_e}\right)^{-1/2}\left(\frac{T}{{}^\circ K}\right)^{-3/2} \tag{20}$$

is the mean adiabaticity parameter, m_e is the electron mass, $\bar{v} = \sqrt{T/m}$, and $\bar{b} = e^2/T$. For large $\bar{\kappa}$, $E_G \gg T$, indicating that superthermal collisions dominate the equipartition rate.

By using the method of steepest descents, the area under the Gamow peak in the integral of Eq. (15) can be determined, yielding

$$\nu_0 = 4\sqrt{2}n\bar{v}\bar{b}^2 I(\bar{\kappa}), \tag{21}$$

where

$$I(\bar{\kappa}) = \frac{\pi}{4}\frac{s(\kappa_G)}{\sqrt{10E_G/T}}e^{-5E_G/3T} \tag{22}$$

and $\kappa_G = \kappa(E_G) = (2/3\pi)E_G/T$. The function $I(\bar{\kappa})$ has been carefully evaluated using both numerical and analytical methods,[15] and the resulting rate ν is shown in Fig. 1. Also shown in the figure are experimental measurements of the equipartition rate, measured in a pure electron plasma over a range of temperatures.[16] At low temperature where $\bar{\kappa} > 1$, the predicted exponential suppression of ν is evident.

III. THE WEAK SCREENING REGIME

The previous theory for ν neglected the effects of plasma screening on the equipartition rate: A bare Coulomb interaction was employed when calculating $\Delta v_{\perp}^2$. To account for the effect of plasma screening, we will follow the argument of Salpeter as applied to nuclear reaction rates in astrophysical conditions, focusing first on the case in which the screening is weak, i.e., where $\Gamma \ll 1$. Salpeter's argument works here because, just as for nuclear reactions, equipartition is dominated by superthermal collisions with energy E_G for which the distance of closest approach e^2/E_G is much smaller than a mean interparticle spacing a. Using Eq. (19) for E_G implies that $e^2/E_G \ll a$ when

$$\bar{\kappa}^{2/5} \gg \Gamma, \tag{23}$$

which is valid when the plasma is strongly magnetized and $\Gamma < 1$. For such close collisions, evaluation of $\Delta v_{\perp}^2$ using an
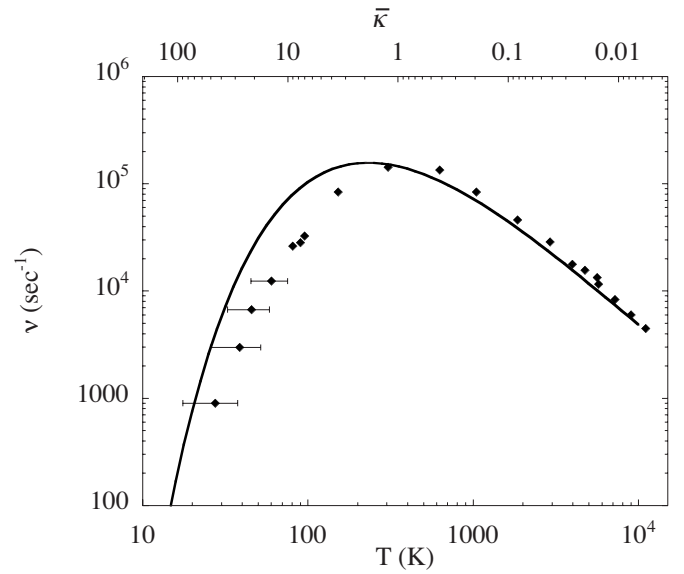

FIG. 1. Adapted from Refs. [15] and [16]. Equipartition rate vs temperature (lower x axis) and $\bar{\kappa}$ (upper x axis) for a pure electron plasma with $B = 6.13$ T, $n = 8 \times 10^8$ cm^{-3}. Dots: Experimental results. Line: Eq. (21).

unscreened two-body Coulomb interaction via Eq. (8) is a good approximation.

However, in the presence of screening, the orbital energy equation, Eq. (9), must be modified. Following Salpeter, we replace it by

$$\frac{\mu}{2}\dot{z}^2 + \phi(\sqrt{\rho^2 + z^2}) = E_{\parallel}, \tag{24}$$

where for ϕ we use a Debye-screened interaction,

$$\phi(r) = \frac{e^2}{r}e^{-r/\lambda_D}, \tag{25}$$

where $\lambda_D^2 \equiv T/4\pi me^2$. We may further simplify the expression for $\dot{z}(t)$ by noting that the contribution of $z(t)$ to the orbit integral in Eq. (24) is dominated by the close approach of $z(t)$ to the origin, where $|z| \ll \lambda_D$. During the close collision, we can Taylor expand $\phi(r)$ in Eq. (24), obtaining

$$\frac{\mu}{2}\dot{z}^2 + \frac{e^2}{\sqrt{\rho^2 + z^2}} = E_{\parallel} + \frac{e^2}{\lambda_D}. \tag{26}$$

That is, a colliding pair starting at infinite separation with relative kinetic energy $E_{\parallel}$ picks up extra kinetic energy e^2/λ_D compared to what it has for no screening, and suffers a stronger collision as a result. This extra energy comes from the attractive potential of the Debye shielding cloud. However, the close collisional dynamics itself is still unscreened. Therefore, we may still employ Eq. (15), the only difference being that the relative kinetic energy is shifted by e^2/λ_D according to Eq. (26),

$$\nu = \int_0^\infty \frac{dE_{\parallel}}{T}e^{-E_{\parallel}/T}\sigma(E_{\parallel} + e^2/\lambda_D), \tag{27}$$

where this expression for ν is valid in the weak-screening regime $\Gamma \ll 1$. Furthermore, since the integrand is dominated

by the Gamow peak, we can make a change of variables from $E_\parallel$ to $E_\parallel + e^2/\lambda_D$ without worrying about the effect of this on the integration limits. This variable change yields

$$\nu = e^{e^2/\lambda_D T}\nu_0, \quad \Gamma \ll 1, \tag{28}$$

where ν_0 is the unscreened result given by Eq. (21). The multiplicative factor $f = e^{e^2/\lambda_D T}$, valid only for $\Gamma \ll 1$, enhances the unshielded equipartition rate ν_0, and is exactly the same as the enhancement factor appearing in the theory of nuclear reactions in the weak-screening regime.[2]

Equation (28) implies that Debye shielding enhances the equipartition (or nuclear reaction) rate. This is opposite to one's usual intuition for binary collisions in a weakly coupled plasma, for which the Debye length cuts off the range of the interaction, so that Debye shielding leads to a (logarithmic) *reduction* in the collision rate. However, almost all of these collisions play no role in the processes considered here, as their impact parameters are too large. The important collisions here are close collisions with impact parameters much smaller than λ_D. As we have seen, the probability of such collisions is enhanced rather than decreased by Debye shielding.

This analysis, while straightforward, has several apparent weaknesses. For instance, it is only valid in the weak screening regime where f is nearly unity. Also, the use of an equilibrium Debye-screening potential would not at first glance appear to be a correct description of collisions between superthermal particles. Some authors have attempted to rectify this apparent flaw by employing "dynamical screening" theories to account for velocity dependence of the screening potential, and have obtained quite different results for the enhancement factor f as a result.[19] However, more careful analysis shows that the use of equilibrium screening potentials is correct. Nevertheless, it would be useful if the enhancement could be measured experimentally under controlled laboratory conditions.

IV. THE STRONG SCREENING REGIME

When the plasma is strongly coupled with $\Gamma \gtrsim 1$, the previous theory based on Debye screening must be modified. However, when

$$1 \lesssim \Gamma < \bar{\kappa}^{2/5}, \tag{29}$$

a theory based on screened two-body collisions is still justified because, according to Eq. (19), $e^2/E_G \ll a$, so the most important collisions are close two-body collisions with surrounding particles relatively distant. We can estimate the screening factor f in this strong-screening regime by noting that, when $\Gamma \gtrsim 1$, the Debye screening cloud around the reacting pair is replaced by a correlation hole with radius of order a. Particles moving toward the center of the hole pick up extra kinetic energy of order e^2/a due to the hole's attractive potential. We can estimate this effect by replacing Eq. (15) by

$$\nu \cong \int_0^\infty \frac{dE_\parallel}{T} e^{-E_\parallel/T} \sigma(E_\parallel + e^2/a), \tag{30}$$

where $\sigma(E_\parallel)$ is the same differential rate used in unscreened collisions. Changing integration variables to $E_\parallel + e^2/a$ then immediately leads to

$$\nu \cong e^\Gamma \nu_0. \tag{31}$$

Therefore in the strong screening regime the rate enhancement factor is roughly $f \sim e^\Gamma$, which is much larger than unity if $\Gamma > 1$. So, equipartition and nuclear fusion are predicted to occur at greatly enhanced rates when the plasma is in the strong screening regime.

A more rigorous derivation of the enhancement factor (Ref. 20) using a Green–Kubo expression for the equipartition rate proves that in the weak and strong screening regimes,

$$\nu = f(\Gamma)\nu_0, \tag{32}$$

and provides an expression for f in terms of partition functions,

$$f(\Gamma) = V Z_{U_{N-1}}(n)/Z_{U_N}(0), \tag{33}$$

where $Z_{U_N}(n)$ is the configurational portion of the canonical partition function for a system of N charges, n of which have charge $2e$. This expression is identical to one derived previously for nuclear reactions in the strong and weak screening regimes.[9] For $\Gamma \ll 1$ it matches the weak screening result, Eq. (28). For $\Gamma > 1$ the expression has been evaluated by different authors using Monte Carlo methods.[7,8,10–13] Two such expressions are given below, valid for $\Gamma \gtrsim 1$, taken from Refs. 10 and 7, respectively,

$$\ln f(\Gamma) = 1.132\Gamma - 0.0094\Gamma \ln \Gamma, \tag{34}$$

$$\ln f(\Gamma) = 1.056299\Gamma + 1.039957\Gamma^{0.323064}$$
$$- 0.545823 \ln \Gamma - 1.1323. \tag{35}$$

At large Γ, $\ln f$ is roughly linear in Γ, as expected from the estimate of Eq. (31).

V. SIMULATIONS

In order to test whether strong screening effects are observable in measurements of energy equipartition, we have performed molecular-dynamics simulations of the equipartition of a Penning trap plasma for N identical charges, where $N=200$ or 512.[20] For the $N=200$ simulations, the plasma is a prolate spheroid in a quadratic trap potential ϕ_{Trap} of the form

$$\phi_{\text{Trap}}(\mathbf{r}) = \tfrac{1}{2}m\omega_z^2(z^2 + \beta(x^2 + y^2)), \tag{36}$$

where the trap parameter $\beta = 2.41$. Here ω_z is the single-particle axial bounce frequency. In the simulations, time is scaled to ω_z and length to $a_0 \equiv (e^2/m\omega_z^2)^{1/3}$, which is roughly an interparticle spacing for a spherical plasma. For the $N=512$ simulations, $\beta=1$ and the plasma is spherical. For simplicity, trap electrodes are assumed to be far from the plasma, so that image charges can be neglected. In such a plasma, the

plasma frequency $\omega_p \equiv \sqrt{4\pi e^2 n/m}$ is related to ω_z and β via the relation[21]

$$\omega_p^2 = (2\beta+1)\omega_z^2, \tag{37}$$

which implies that the unscreened equipartition rate, Eq. (21), is

$$\nu_0 = \frac{\sqrt{2}}{\pi}\omega_z \frac{(2\beta+1)}{\hat{T}^{3/2}}I(\bar{\kappa}), \tag{38}$$

and the coupling parameter is

$$\Gamma = \left(\frac{2\beta+1}{3}\right)^{1/3} \Bigg/ \hat{T}. \tag{39}$$

Here $\hat{T} = T/m\omega_z^2 a_0^2$ is the temperature in simulation units. Also, $\bar{\kappa}$ is

$$\bar{\kappa} = \sqrt{2}\frac{-\Omega_c}{\omega_z}\hat{T}^{-3/2}. \tag{40}$$

For the first simulation with $N = 200$ and $\beta = 2.41$, the cyclotron frequency was $\Omega_c = 30\omega_z$, which implies $\Omega_c/\omega_p = 12.4$, $\bar{\kappa} = 42.4/\hat{T}^{3/2}$, and $\Gamma = 1.25/\hat{T}$. A fourth-order Runge–Kutta method was used with a fixed time step size of $6 \times 10^{-4}\omega_z^{-1}$. Over the course of a typical run of 10^7 time steps, energy was conserved to within one part in 10^6. As a test of accuracy, the time step size was reduced by a factor of 2, and while this led to a different time evolution for charges in the system (as one would expect for a chaotic system), the gross evolution (neglecting fluctuations) of parallel and perpendicular temperatures was unaffected. These temperatures were measured in the usual manner, as

$$T(t) = \sum_{i=1}^{N} m\mathrm{v}_{\parallel i}^2(t) \tag{41}$$

and

$$T_\perp(t) = \sum_{i=1}^{N} m\mathrm{v}_{\perp i}^2(t)/2. \tag{42}$$

The initial condition was chosen so that $T_\perp \gg T$ (see Fig. 2). Initially, there was no measurable equipartition between $T_\perp$ and T.

The parallel temperature was then instantaneously increased by multiplying all parallel velocities by a factor of 3. Again, no equipartition was observed to occur over the course of a 10^7 time step run. Parallel velocities were then multiplied by a factor of 2, so that $\hat{T} \sim 0.2$ ($\Gamma \sim 6$ and $\bar{\kappa} \sim 470$), and this eventually led to equipartition (Fig. 2). The observed equipartition rate ν_{sim} was then measured using Eq. (14),

$$\nu_{\mathrm{sim}} = \frac{dT_\perp/dt}{T - T_\perp}. \tag{43}$$

Since both $T_\perp$ and T fluctuate in these finite N simulations, evaluation of $dT_\perp/dt$ must be performed carefully in order to minimize artifacts caused by the fluctuations. Various methods were tried, such as fitting an entire $T_\perp(t)$ run to different smooth analytic functions. In most cases, however, the best
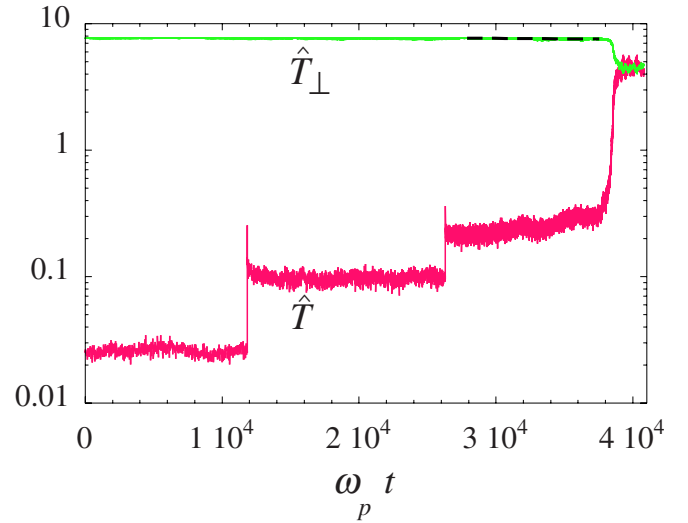

FIG. 2. (Color online) Temperature vs time for the simulation shown by the red lines in Fig. 3. The dashed line is a linear fit to $T_\perp(t)$ discussed in the text.

results were obtained by fitting $T_\perp$ to line segments over short time intervals of roughly $20\omega_p^{-1}$.

This algorithm yielded the ν_{sim} vs T curve given by the red dots in Fig. 3. For this run we also fit the initial equipartition to a single straight line (the dashed line in Fig. 2), yielding the rate given by the thin red horizontal line in Fig. 3. Also in this figure we plot the predicted unshielded rate ν_0 of Eq. (38) and the rate ν with shielding from Eq. (32), using Eq. (35) for $f(\Gamma)$. The measured rate is substantially larger than the unshielded rate ν_0 except at large T, where $\Gamma < 1$. Moreover, ν_{sim} does track the shielded prediction for ν within a factor of 2–3.

While the agreement between theory and simulation is gratifying, it is also rather surprising when looked at from the following perspective. When equipartition began in the simulation, at $\hat{T} \sim 0.2$ and $\bar{\kappa} \sim 470$, the Gamow energy was $E_G \cong 14T$ according to Eq. (19). This is so far out on the tail
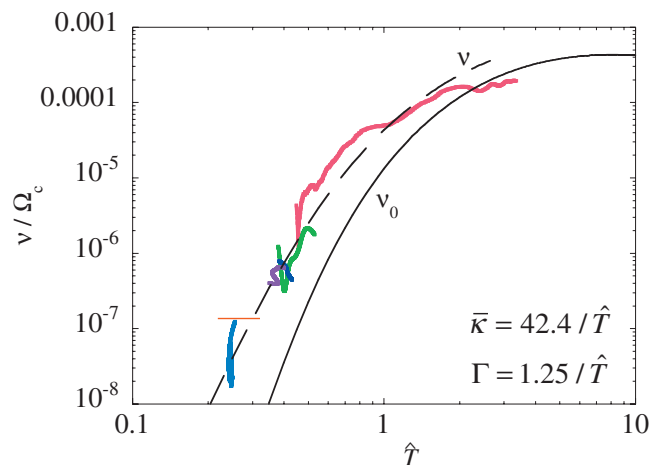

FIG. 3. (Color) Equipartition rate vs scaled temperature for several simulations, compared to theory with (dashed) and without (solid) screening. The enhancement factor is modeled by Eq. (35).
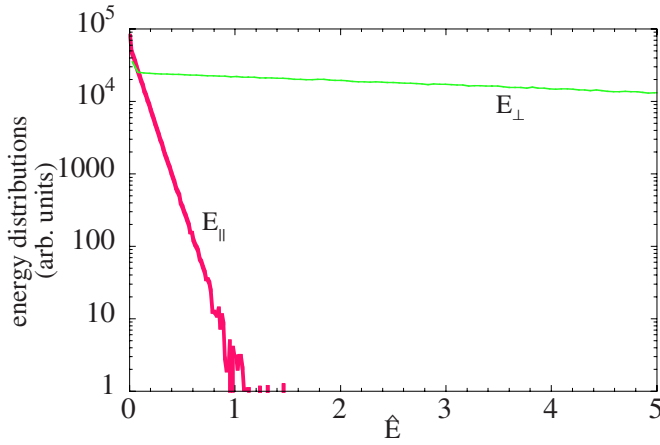
FIG. 4. (Color online) Parallel and perpendicular kinetic energy distributions for the run displayed in Fig. 2, averaged over times $16200 < \omega_p t < 26200$.

FIG. 5. (Color online) Temperature vs time for the simulation shown by the purple curve in Fig. 3, with $T > T_\perp$.

of the Maxwellian that, for $N=200$ particles, it takes $\ln(2)/(Ne^{-E_G/T})=6000$ realizations of the particle velocities for there to be a 50% chance of at least one particle having energy E_G or larger. Estimating the velocity correlation time as roughly ω_p^{-1} in this strongly coupled plasma, we see that it is not guaranteed that the tail of the Maxwellian will be populated beyond E_G over the time of $\sim 5000\omega_p^{-1}$ that equipartition initially occurs.

Put another way, it is not clear that, for such unlikely events as particles having energy E_G, a Maxwellian velocity distribution is the correct description. Before equipartition begins, Fig. 4 shows that both parallel and perpendicular velocity distributions are Maxwellian to an excellent approximation, but the parallel distribution cannot be measured out to $E=E_G$. On the other hand, when equipartition is proceeding in earnest, i.e., at $\hat{T} \gtrsim 0.4$, then $\bar{\kappa}$ and E_G are smaller, $\bar{\kappa} \lesssim 170$ and $E_G/T \lesssim 9.5$. Now the number of uncorrelated realizations required for at least one particle to have $E > E_G$ with 50% probability is less than 50, so the velocity distribution should be populated up to and even somewhat beyond E_G during this portion of the evolution. Under these conditions, the theory has a better chance of success.

The best test of the theory in these circumstances is to simply repeat the simulations for different initial conditions. Several simulations were performed for the same values of β, N, and Ω_c/ω_z but with $T_\perp \ll T$ initially. An example of one such run is shown in Fig. 5. Now T decreases as the temperatures equilibrate, which reduces the equipartition rate so that full equipartition does not occur. This is actually useful because the slower variation in T and $T_\perp$ allows longer averaging and hence a better signal-to-noise ratio when determining $dT_\perp/dt$. The measured rates from three such runs (blue, green, and purple curves in Fig. 3) still agree with theory including strong screening effects, within the measurement error.

As a further test, two more runs were performed with $N=512$, $\beta=1$, and $\Omega_c/\omega_z=10$. For these parameters, $\bar{\kappa}=14.1/\hat{T}^{3/2}$ and $\Gamma=1/\hat{T}$. The measured and predicted rates are displayed in Fig. 6, and again there is agreement with

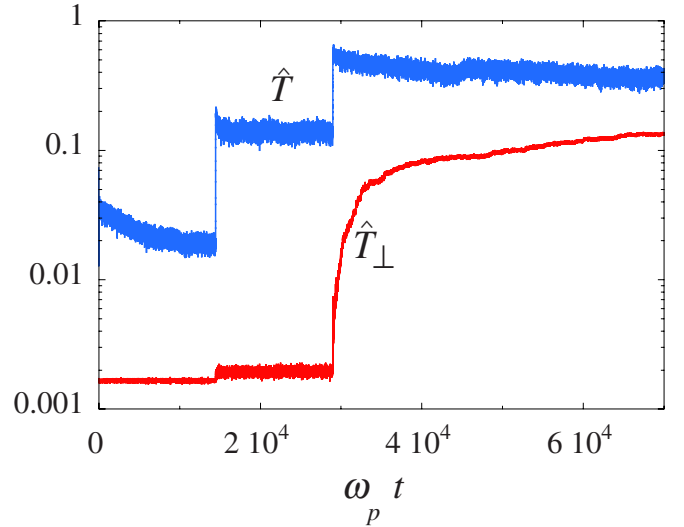theory, within the errors. Note, however, that the predicted rate displays an unphysical increase as $\hat{T}$ decreases. This is because, for these parameters, inequality (23) is not satisfied for $\hat{T} < 0.17$.

In this low-temperature regime, the distance of closest approach for particles at the Gamow energy is larger than an interparticle spacing a, so the strong screening theory based on close two-body collisions does not apply. The many-body collision regime $\Gamma > \kappa^{2/5} \gg 1$ for which $e^2/E_G > a$ is referred to here as the "pycnonuclear regime," in analogy to the high-density regime considered in the theory of screened nuclear reactions.[4,6,8,12,13] This regime will be considered in more detail in Sec. VI.

An "experimental" measurement of the rate enhancement function $f(\Gamma)$ can be extracted from the preceding measurements of $\nu_{\text{sim}}(T)$ by simply taking $f=\nu_{\text{sim}}/\nu_0$ according to Eq. (32). This ratio is plotted in Fig. 7 for each simulation,
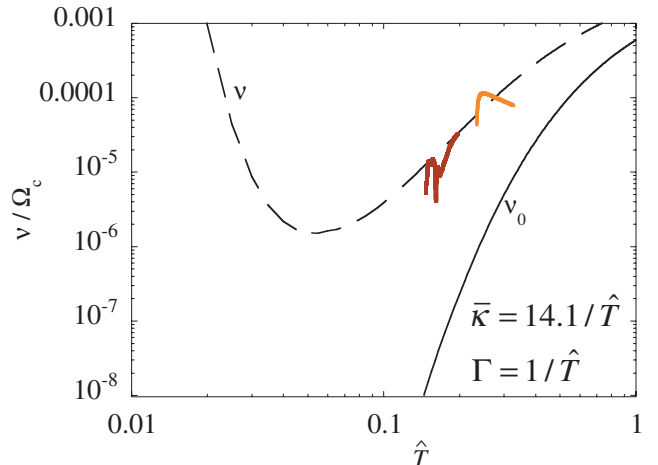

FIG. 6. (Color) Equipartition rate for two $N=512$ simulations, compared to theory with (dashed) and without (solid) plasma screening. The increase in ν below $\hat{T}=0.1$ is unphysical.
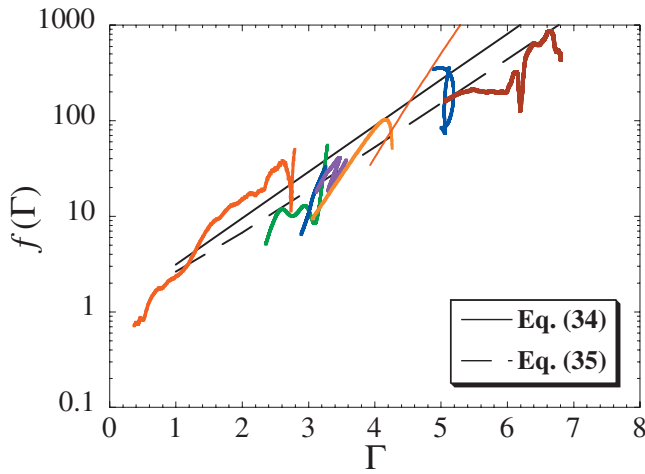
FIG. 7. (Color) The enhancement factor $f(\Gamma)$ extracted from the previous simulations, and compared to theory. The colors correspond to those in Figs. 3 and 6.
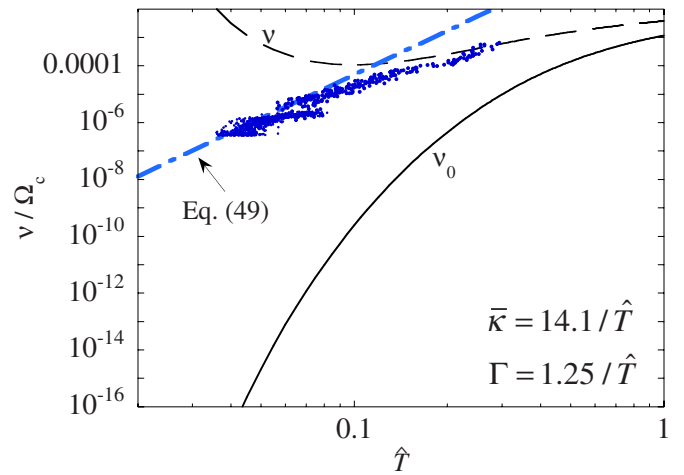

FIG. 8. (Color online) A simulation of equipartition in the classical pycno-nuclear regime $\Gamma > \bar{\kappa}^{2/5}$, compared to theory assuming strong screening (dashed), no screening (solid), and an estimate of phonon-phonon interactions (dot-dashed).

and compared to Eqs. (34) and (35). The measured enhancement factor is in reasonable agreement with the theories, and the simulations cannot distinguish between them, except possibly for the largest Γ run. However, this large Γ run is on the edge of the pycnonuclear regime, which probably affects the results. More simulations with higher accuracy are needed to distinguish between the theories for $f(\Gamma)$. As far as we know, this is the first time that theories for the screening enhancement factor have been tested in the strong screening regime.

VI. THE PYCNONUCLEAR REGIME

In the pycnonuclear regime, the temperature is sufficiently low so that

$$\Gamma > \bar{\kappa}^{2/5} \gg 1. \tag{44}$$

The Gamow peak in the equipartition rate occurs for collisions with impact parameters greater than an interparticle spacing, i.e., $e^2/E_G > a$. In this regime, the previous strong-shielding analysis based on binary collisions fails, as can be seen by the unphysical increase in ν as temperature decreases in Fig. 6.

We have carried out simulations of equipartition in the pycnonuclear regime. The results of one such simulation are shown in Fig. 8. For this simulation, $N=200$, $\beta=2.41$, and $\Omega_c/\omega_z=10$. This implies $\Gamma=1.25/\hat{T}$, $\Omega_c/\omega_p=4.14$, and $\bar{\kappa}=14.1/\hat{T}^{3/2}$. For $\hat{T}>0.12$, the simulation is in the strong-shielding regime and the measured equipartition rate approaches Eq. (32), as expected. For $\hat{T}<0.12$, the simulation is in the pycnonuclear regime, and the measured rate diverges from the strong-shielding theory. At the lowest temperatures, the measured equipartition rate is over 10^{10} times larger than the uncorrelated rate ν_0, and 10^4 times smaller than the strong-shielding prediction.

Currently, no theory explains these results in detail. Previous theories of the pycnonuclear regime, developed for nuclear reactions, necessarily involve quantum effects, and so do not apply here. For nonresonant nuclear reactions, the Gamow energy E_N is on the order of $E_N \sim T(b/r^*)^{1/3}$, where

$r^*=\hbar/me^2$ is the nuclear Bohr radius. The pycnonuclear regime $e^2/E_N > a$ can then be expressed as $\hbar\omega_p > T$, where ω_p is the ion plasma frequency.[12] Thus, for nuclear reactions the pycnonuclear regime requires that lattice vibrations are quantum-mechanical. In our simulations, however, equipartition occurs in a classical pycnonuclear regime for which $\hbar\omega_p \ll T$ is assumed. This classical pycnonuclear regime has no direct analogue in the theory of screened nuclear reactions. Nevertheless, understanding the physics behind the large observed rate enhancement in our classical pycnonuclear simulations may provide some insights into the quantum pycnonuclear processes in nuclear reactions.

One possible explanation for the observed rate involves collective phonon "collisions." When a description of interactions based on binary collisions fails, it may be more appropriate to describe the interactions as collective processes involving the emission and absorption of phonons. In a strongly magnetized non-neutral plasma, the phonons fall into three frequency regimes: Cyclotron phonons with frequencies of order Ω_c, plasma phonons with frequencies of order ω_p, and $\mathbf{E} \times \mathbf{B}$ drift phonons with frequencies of order ω_p^2/Ω_c.[22] In the collective picture of equipartition, breaking the adiabatic invariant involves the creation or annihilation of a cyclotron phonon, whose energy is then distributed among several lower-frequency phonons. The most likely process is one for which the smallest number of lower-frequency phonons are emitted, implying that $\mathbf{E} \times \mathbf{B}$ drift phonons are not involved, only plasma and cyclotron phonons. Energy conservation then implies that M plasma phonons are created when a cyclotron phonon is annihilated, where M is roughly given by

$$\Omega_c = M\omega_p. \tag{45}$$

The rate for such a process can be estimated from the exact Green–Kubo expression for the equipartition rate,[23]

$$\nu = \frac{1}{2NT_\perp T} \int_{-\infty}^{\infty} \langle \dot{E}_\perp(t)\dot{E}_\perp(0)\rangle dt, \tag{46}$$

where $\dot{E}_\perp(t)$ is the rate of change of total perpendicular kinetic energy. A rough estimate of $\dot{E}_\perp$ due to collective motions is

$$\dot{E}_\perp \sim Ne^2 \frac{\mathbf{v}_\perp(t)\cdot\mathbf{a}}{|a^2+(a+\Delta z)^2|^{3/2}}, \tag{47}$$

where $\mathbf{a}$ is the displacement between nearest neighbors in the strongly coupled plasma, $\mathbf{v}_\perp(t)$ is the perpendicular velocity associated with cyclotron motion, and $\Delta z(t)$ is the small parallel displacement associated with plasma phonons. The time integral in Eq. (46) is then dominated by resonant terms where $1/|a^2+(a+\Delta z(t))^2|^{3/2}$ has time-variation of the same frequency scale as Ω_c. Since $\Delta z(t)$ is small and varies relatively slowly, at frequency ω_p, we can estimate this effect by Taylor expansion of $1/|a^2+(a+\Delta z(t))^2|^{3/2}$ up to order M, where resonance occurs,

$$\dot{E}_\perp \sim \frac{(M/2)!!}{(M/2)!} Ne^2 \frac{\mathbf{v}_\perp(t)\cdot\mathbf{a}}{a^3}\left(\frac{\Delta z(t)}{a}\right)^M. \tag{48}$$

An average over harmonic lattice vibrations, for which $\langle(\Delta z/a)^M\rangle \sim (M/2)! \times (T/m\omega_p^2)^{M/2}$, then yields

$$\nu \sim \frac{\omega_p^2}{\Omega_c \Gamma} e^{-M\ln(\beta\Gamma/M)}, \tag{49}$$

where β is a constant of order unity. This crude estimate for the equipartition rate is exponentially small since the ratio of cyclotron to plasma frequencies $M=\Omega_c/\omega_p$ is greater than unity. Equation (49) is plotted in Fig. 8, taking $\beta=1$. It is a surprisingly good fit to the data, indicating that a more care-ful analysis of this collective picture of equipartition is warranted.

[1] E. Schatzman, J. Phys. Radium **9**, 46 (1948).
[2] E. E. Salpeter, Aust. J. Phys. **7**, 373 (1954).
[3] A. G. Cameron, Astrophys. J. **130**, 916 (1959).
[4] E. E. Salpeter and H. Van Horn, Astrophys. J. **155**, 183 (1969).
[5] A. Alastuey and B. Jancovici, Astrophys. J. **226**, 1034 (1978).
[6] S. Ichimaru, Rev. Mod. Phys. **65**, 255 (1993).
[7] H. DeWitt and W. Slattery, Contrib. Plasma Phys. **39**, 97 (1999).
[8] S. Ichimaru and H. Kitamura, Phys. Plasmas **6**, 2649 (1999).
[9] B. Janovici, J. Stat. Phys. **17**, 357 (1977).
[10] S. Ogata, Astrophys. J. **481**, 883 (1997).
[11] S. Ogata, H. Iyetomi, and S. Ichimaru, Astrophys. J. **372**, 259 (1991).
[12] A. Chugunov, H. E. DeWitt, and D. G. Yakovlev, Phys. Rev. D **76**, 025028 (2007).
[13] L. R. Gasques, A. V. Afanasjev, E. F. Aguilera, M. Beard, L. C. Chamon, P. Ring, M. Wiescher, and D. G. Yakovlev, Phys. Rev. C **72**, 025806 (2005).
[14] T. M. O'Neil and P. G. Hjorth, Phys. Fluids **28**, 3241 (1985).
[15] M. E. Glinsky, T. M. O'Neil, M. N. Rosenbluth, K. Tsuruta, and S. Ichimaru, Phys. Fluids B **4**, 1156 (1992).
[16] B. R. Beck, J. Fajans, and J. H. Malmberg, Phys. Rev. Lett. **68**, 317 (1992).
[17] M. J. Jensen, T. Hasegawa, J. J. Bollinger, and D. H. E. Dubin, Phys. Rev. Lett. **94**, 025001 (2005).
[18] F. Anderegg, D. H. E. Dubin, C. F. Driscoll, and T. M. O'Neil, Bull. Am. Phys. Soc. **51**, 249 (2006).
[19] J. N. Bahcall, L. S. Brown, A. Gruzinov, and R. F. Sawyer, Astron. Astrophys. **383**, 291 (2002); N. Shaviv and G. Shaviv, Astrophys. J. **558**, 925 (2001).
[20] D. H. E. Dubin, Phys. Rev. Lett. **94**, 025002 (2005).
[21] D. H. E. Dubin and T. M. O'Neil, Rev. Mod. Phys. **71**, 87 (1999).
[22] D. H. E. Dubin, Phys. Rev. E **53**, 5268 (1996).
[23] This argument is adapted from S.-J. Chen, Ph.D. thesis, University of California at San Diego (1994).